ELSEVIER

Journal of Power Sources 114 (2003) 244–252

JOURNAL OF POWER SOURCES

www.elsevier.com/locate/jpowsour

Effect of synthesis conditions on electrochemical properties of $LiNi_{1-y}Co_yO_2$ cathode for lithium rechargeable batteries

B.J. Hwang*, R. Santhanam, C.H. Chen

Microelectrochemistry Laboratory, Department of Chemical Engineering, National Taiwan University of Science and Technology, 43 Keelung Road, Section 4, 106 Taipei, Taiwan, ROC

Received 9 July 2002; accepted 18 October 2002

Abstract

$LiNi_{1-y}Co_yO_2$ samples are prepared by a sol–gel method at various cobalt concentrations (y-value) by sintering at 800 °C for a period of 10 h. An X-ray diffraction technique is used to examine the structural properties of the samples. The sample with a y-value of 0.25 has the largest initial discharge capacity and shows the best cycling performance. It is concluded that this performance results from better hexagonal ordering, crystallinity, and smaller particle size with good particle-size distribution compared with other samples. $Li_xNi_{0.75}Co_{0.25}O_2$ samples with different lithium content are also prepared and it is found that $Li_{1.05}Ni_{0.75}CO_{0.25}O_2$ shows the best electrochemical performance. This suggests that the presence of excess lithium prevents the exchange of Ni^{2+} ions at lithium sites.

Keywords: Capacity retention; Lithium-ion battery; Lithium nickel oxides; *R*-factor; Sol–gel process; Synthesis conditions

1. Introduction

Rechargeable lithium batteries based on layered cathode phases, viz. $LiCoO_2$ and $LiNiO_2$, have received a great deal of attention in recent years [1–5]. Both these materials have a layered rocksalt structure with a rhombohedral $R3$-m space group. Mostly, $LiCoO_2$ has been used as a positive electrode (cathode) in rechargeable lithium cells presently in the market. Nevertheless, this is not an attractive cathode material for lithium batteries due to its high cost and toxicity. For these reasons, $LiNiO_2$ has been considered as a promising cathode material. It is extremely difficult, however, to synthesise stoichiometric $LiNiO_2$ due to the high-temperature preparation conditions that lead to the formation of $Li_{1-x}Ni_{1+x}O_2$ [6,7]. This non-stoichiometry or lithium-deficient material has rather poor electrochemical performance because excess nickel ions are occupying the lithium sites and hindering the diffusion of lithium during charging and discharging [8–10]. Hence, excess lithium is often required during preparation to reduce the lithium deficiency in the final material.

Usually, $LiNiO_2$ and its derivatives are synthesised by the solid-state reaction method which is a time-consuming process involving high-temperature sintering and extended grinding of starting material like hydroxides, nitrates and carbonates [11–13]. This method also has several other disadvantages, namely inhomogeneity, irregular morphology, larger particle size, broader particle-size distribution, and poor control of stoichiometry. Several solution methods have been developed to obtain sub-micron particles of uniform morphology with a arrow size distribution and good homogeneity [14–16].

The starting materials and synthesis processes have an effect on the electrochemical characterisation of $LiNiO_2$ and its derivatives. By optimising the synthesis conditions, its electrochemical and cycling behaviour can be improved. A great deal of research has been undertaken on dopant materials to overcome the problems associated with $LiNiO_2$ [17]. Doped $LiNiO_2$ may possess better electrochemical properties than $LiNiO_2$ or $LiCoO_2$. Gover et al. [18] prepared $LiNiO_2$ doped with 20 wt.% Co and showed the relationship between synthesis temperature, structure and electrochemical properties. Alcantara et al. [19] reported that a synthesis temperature of 750 °C was required to prepare good samples of $Li_{1-x}(Ni_yCo_{1-y})_{1+x}O_2$. Single-phase $LiNi_{0.8}Co_{0.2}O_2$ samples were prepared by Saadoune and Delmas at 800 °C [20]. According to Fujita et al. [21],

* Corresponding author. Tel.: +886-2-27376624; fax: 886-2-27376644.
E-mail address: bjh@ch.ntust.edu.tw (B.J. Hwang).

0378-7753/02/$ – see front matter
PII: S0378-7753(02)00584-0

$LiNi_{0.85}Co_{0.15}O_2$ can be prepared at temperatures as low as 400 °C. Recently, the effects of sintering temperature on the structure of the layered phase were reported [22]. Different research groups have studied the electrochemical performance of $LiNiO_2$ with various percentages of Co-doping [23–27]. This work suggests that the electrochemical characteristics are sensitive to the microstructure of the electrode material, which varies with the synthesis conditions.

In this investigation, a $LiNi_{1-y}Co_yO_2$ sample is synthesised with different y-values, as well as a $Li_xNi_{1-y}Co_yO_2$ sample with different x-values, using a sol–gel method under various conditions. The relationship between the synthesis conditions and the electrochemical properties of the prepared $LiNi_{1-y}Co_yO_2$ and $Li_xNi_{1-y}Co_yO_2$ samples, is also examined.

2. Experimental

Stoichiometric $LiNi_{1-y}Co_yO_2$ and non-stoichiometric $Li_xNi_{1-y}Co_yO_2$ powders were synthesised by the sol–gel method using citric acid as a chelating agent [28,29]. Stoichiometric amounts of lithium acetate ($Li(CH_3COO)\cdot 2H_2O$), nickel acetate ($Ni(CH_3COO)_2\cdot 4H_2O$), and cobalt nitrate ($Co(NO_3)_2\cdot 6H_2O$) were dissolved in distilled water and mixed with aqueous solution of citric acid. The resulting solution was mixed with a magnetic stirrer at 80–90 °C for 5–6 h to obtain a clear viscous gel. The gel was dried in a vacuum oven at 140 °C for 24 h. All the $LiNi_{1-y}Co_yO_2$, and $Li_xNi_{1-y}Co_yO_2$ compounds were ground and calcined at 750–900 °C after pre-calcining the obtained precursor at 450 °C. During heating and cooling, the variation of the temperature was fixed at 2 °C min^{-1}.

The Li, Co and Ni contents in the resulting materials were analysed using an inductively coupled plasma/atomic emission spectrometer (ICP/AES; Kontron S-35). Phase purity was verified by means of powder X-ray diffraction (XRD; Rigaku D/max-b) using Cu Kα radiation. The particle morphology of the powders after calcination was examined with scanning electron microscopy (SEM; Hitachi S-4100). Electrochemical characterisation was carried out with coin-type cells. The cathode was prepared by mixing 85:3.5:1.5:10 (w/w) ratio of active material, carbon black, KS6 graphite and polyvinylidene fluoride binder, respectively, in *N*-methyl pyrrolidinone. The resulting paste was applied to a aluminium current-collector. The entire assembly was dried under vacuum overnight and then heated in an oven at 120 °C for 2 h. Lithium metal (Aldrich) was used as an anode and a polypropylene separator was used to separate the anode and the cathode. $LiPF_6$ (1.0 M) dissolved in a 1:1 mixture of ethylene carbonate (EC) and diethyl carbonate (DEC) was used as an electrolyte. The cells were assembled in an argon-filled dry box where both the moisture and the oxygen contents were <1 ppm. Charge and discharge cycles were carried out at the 0.1*C* rate over a potential range between 3.0 and 4.3 V.

3. Results and discussion

Synthesis conditions must be carefully selected to obtain pure layered $LiNiO_2$ and $LiNi_{1-y}Co_yO_2$ materials since they directly influence the electrochemical characteristics of the materials. In the present work, the sol–gel method is used to synthesise the materials due to its advantage of molecular/ionic scale mixing which can lower the reaction temperature. X-ray diffraction patterns are shown in Fig. 1(a) for $LiNi_{1-y}Co_yO_2$, where $y = 0.05$, 0.10, 0.15, 0.20, 0.25 and 0.30, prepared by the sol–gel method at 800 °C for 10 h. The XRD spectra show that all the samples have a typical layered structure with space group *R*3-*m*. No impurity-related peaks are observed from the XRD pattern for $LiNi_{1-y}Co_yO_2$. All the peaks are identified as the characteristics peaks of $LiNi_{1-y}Co_yO_2$ reported in the X-ray powder data file of JCPDS. Variation of the discharge capacities for $LiNi_{1-y}Co_yO_2$ with cycle number is shown in Fig. 1(b). The cells were subjected to 20 cycles at a rate of 0.1*C* between 3.0 and 4.3 V. Capacity fading is observed for all the samples. $LiNi_{1-y}Co_yO_2$ with $y = 0.25$ has the largest first discharge capacity and exhibits better cycling behaviour than samples with other y-values. The charge and discharge capacities of the selected cycles are summarised in Table 1. Hereafter, the $LiNi_{1-y}Co_yO_2$ sample with $y = 0.25$ is discussed in detail.

In order to evaluate the effect of sintering temperature on electrochemical performance, $LiNi_{0.75}Co_{0.25}O_2$ material was synthesised at different sintering temperatures. The XRD patterns of $LiNi_{0.75}Co_{0.25}O_2$ sintered for 10 h between 750 and 900 °C are shown in Fig. 2. The samples are identified as a layered hexagonal phase with space group *R*3-*m*. Scanning electron micrographs of $LiNi_{0.75}Co_{0.25}O_2$ samples sintered at various temperatures are shown in Fig. 3. The sample sintered at 750 °C consists of particles with a highly amorphous nature. The sample sintered at 850 °C has both large and small crystalline particles. The sample sintered at 900 °C has relatively large particles, but the sample sintered at 800 °C has small crystalline particles of uniform size.

The variation of lattice parameters (c and a), c/a ratio, *R*-factor $[(I_{006} + I_{102})/I_{101}]$, I_{003}/I_{104} ratio and unit-cell volume of the $LiNi_{0.75}Co_{0.25}O_2$ sample with respect to sintering temperature is summarised in Table 2. Even though there are no significant changes in the c, a values and the c/a ratio for the sample sintered at different temperatures, a relatively large increase in the I_{003}/I_{104} ratio is observed for the sample sintered at 800 °C. According to previous results published by Gao et al. [30] an increase in the I_{003}/I_{104} ratio indicates less cation mixing. Moreover, the *R*-factor is relatively lower for the sample sintered at 800 °C. According to Riemers et al. [31], the *R*-factor is inversely proportional to the hexagonal ordering. In other words, the lower the *R*-factor, the higher is the hexagonal ordering and hence the better cycling performance. Furthermore, the unit-cell volume observed for the $LiNi_{0.75}Co_{0.25}O_2$ sample sintered at 800 °C is smaller than that of the samples sintered at other temperatures. Dahn et al. [32] reported that material with

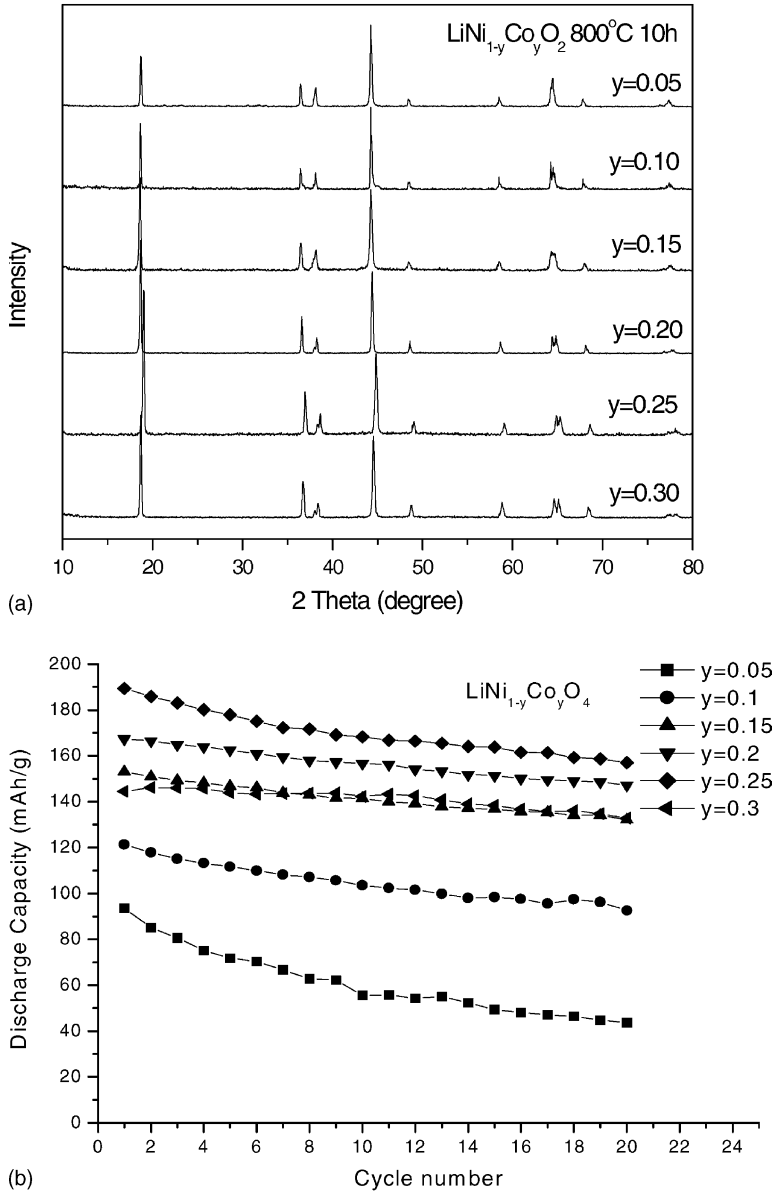

Fig. 1. XRD patterns (a) and discharge capacity vs. cycle number (b) for $LiNi_{1-y}Co_yO_2$ samples with different y-values prepared at 800 °C for 10 h.

more layered characteristics would have lower cell volume. These authors also asserted that the $LiNi_{0.75}Co_{0.25}O_2$ sample sintered at 800 °C has more layered characteristics since it has a lower cell volume than other samples. The splitting between (1 0 8) and (1 1 0) peaks is another important determinant of electrochemical activity. The symmetric splitting observed between these peaks for the $LiNi_{0.75}Co_{0.25}O_2$ sample sintered at 800 °C indicates that this

Table 1
Charge (CC) and discharge (DC) capacities of $LiNi_{1-y}Co_yO_2$ for various y-values

Cycle	$LiNi_{1-y}Co_yO_2$											
	$y = 0.05$		$y = 0.1$		$y = 0.15$		$y = 0.2$		$y = 0.25$		$y = 0.3$	
	CC	DC	CC	DC	CC	DC	CC	DC	CC	DC	CC	DC
1	153.4	93.5	163.2	121.3	227.9	153.1	195.6	167.3	232.0	189.3	184.0	144.5
2	88.2	85.0	118.9	117.9	153.2	150.9	167.8	166.5	189.5	185.8	145.5	146.1
5	72.6	71.8	112.0	111.7	148.5	146.7	164.5	162.5	179.7	177.9	146.7	143.9
10	56.9	55.5	104.5	103.4	141.9	141.4	158.0	156.7	168.9	168.2	144.0	142.2
20	44.3	43.6	94.6	92.6	134.6	132.0	149.1	147.1	158.1	157.0	134.9	132.7

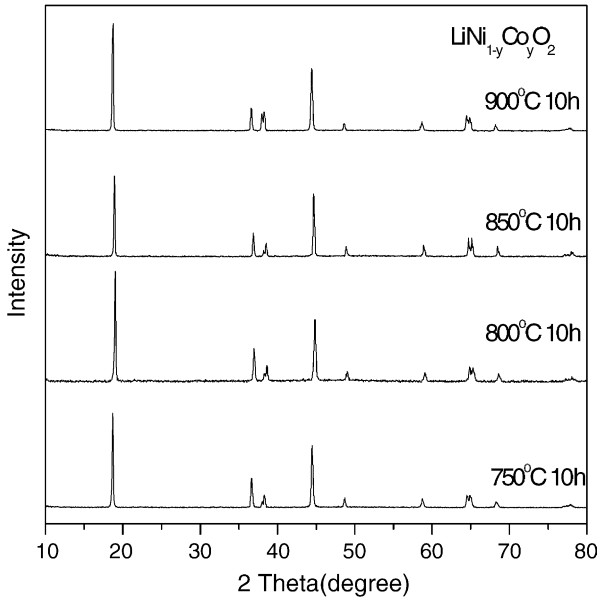

Fig. 2. XRD patterns $LiNi_{0.75}Co_{0.25}O_2$ samples prepared between 750 and 900 °C for 10 h.

sample has less cation disordering and greater layered characteristics (Fig. 2).

The variation of grain size of $LiNi_{0.75}Co_{0.25}O_2$ prepared under various sintering temperatures is shown in Fig. 3. Scherrer's formula was used to determine the grain size (t), i.e.

$$t = \frac{0.9\lambda}{B\cos\theta_B} \quad (1)$$

where λ is the wavelength of the X-ray used, θ_B the Bragg angle of the diffraction peak considered and B the width at an intensity equal to half I_{max} [33]. The grain size is not significantly changed as the temperature is raised from 750 to 800 °C, as shown in Fig. 4. The grain size increases abruptly, however, for samples sintered above 800 °C. All the above mentioned factors, particle/grain size, particle-size distribution, c/a ratio, R-factor, unit-cell volume, and splitting between (1 0 8) and (1 1 0) peaks with respect to sintering temperature would have direct impact on the cycling performance of the $LiNi_{0.75}Co_{0.25}O_2$ sample, as explained below.

The electrochemical results obtained for the sample prepared at 800 °C are given in Fig. 5. For clarity, only selected cycles are shown. The results reveal that all the samples have good electrochemical properties. This is graphically demonstrated in Fig. 6(a), which shows the variation of discharge capacity as a function of sintering temperature for cycles 1, 10 and 20. The variation of discharge capacity as a function of cycle number is given in Fig. 6(b). Capacity fading is found over an extended number of charge and discharge cycles. The electrochemical properties of the 1st and 20th

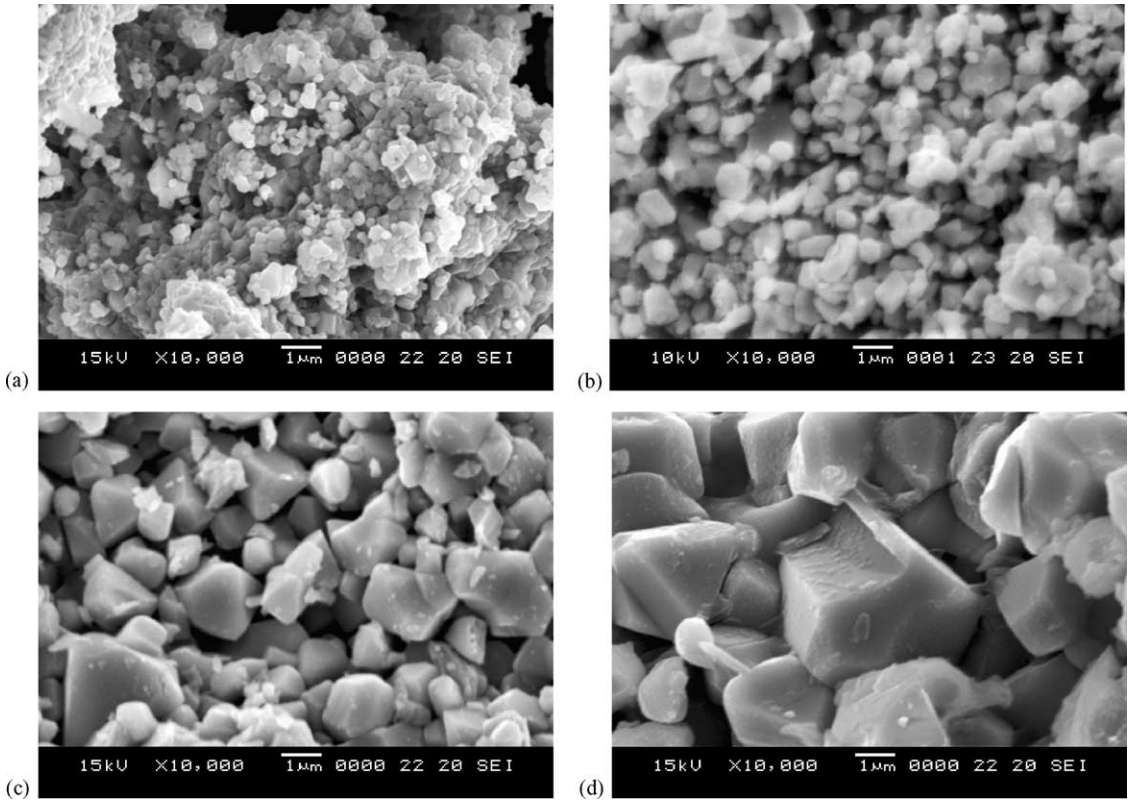

Fig. 3. Scanning electron micrographs of $LiNi_{0.75}Co_{0.25}O_2$ samples prepared at different temperatures for 10 h: (a) 750 °C; (b) 800 °C; (c) 850 °C; (d) 900 °C.

Table 2
Lattice parameters, *c*/*a* values, *R*-factors, I_{003}/I_{104} intensity ratio and unit-cell volume of $LiNi_{0.75}Co_{0.25}O_2$ at various sintering temperatures

Temperature (°C)	*a* (Å)	*c* (Å)	*c*/*a* Ratio	*R*-factor $(I_{006} + I_{102})/I_{101}$	I_{003}/I_{104}	Unit-cell volume (Å^3)
750	2.8715	14.1814	4.94	0.66	1.51	101.2651
800	2.8651	14.1716	4.95	0.54	1.85	100.7472
850	2.8692	14.1739	4.94	0.84	1.27	101.0498
900	2.8693	14.1751	4.94	1.61	1.72	101.0659

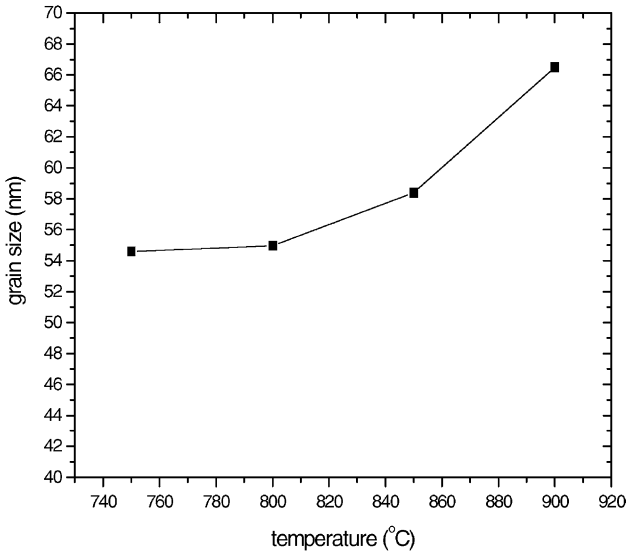

Fig. 4. Variation of grain size of $LiNi_{0.75}Co_{0.25}O_2$ sample prepared at different sintering temperatures.

cycles for a $LiNi_{0.75}Co_{0.25}O_2$ sample prepared at different temperatures sintered for 10 h are presented in Table 3. Interestingly, the $LiNi_{0.75}Co_{0.25}O_2$ sample prepared at 800 °C exhibits the highest initial charge capacity of 232 mAh g^{-1} with 82% capacity retention (189 mAh g^{-1}) during discharge. In a similar study, Gover et al. [22] reported a highest charge capacity of 269 mAh g^{-1} for a sample sintered at 600 °C, but over 40% of the charge capacity was lost on discharge. In their study the Co doping is only 20%; it is 25% in our sample. In the same report [22], it was established, from powder XRD and neutron diffraction studies, that the sample with better 3*a* site order has a higher cycling efficiency. Thus, it is concluded that the sample prepared in this work at 800 °C sintering for 10 h will have better 3*a* site order since it shows initial charge and discharge capacities of 232 and 189.3 mAh g^{-1}, respectively, with 18.4% capacity loss, and 20th charge and discharge capacities of 158 and 157 mAh g^{-1}, respectively, with only 1.1% capacity loss.

It is known that stoichiometric $LiNiO_2$ is extremely difficult to prepare because of the loss of lithium from the host structure due to the high vapour pressure of lithium at high sintering temperature [32]. This leads to the formation of non-stoichiometric $Li_{1-x}Ni_{1+x}O_2$ [7]. Non-stoichiometry is associated with the presence of Ni^{2+} in the 3*a* layer sites which restricts the diffusion of lithium ions within the layers. To date, only a few studies have been reported on the electrochemical performance of non-stoichiometric $Li_xNi_{1-y}Co_yO_2$ [18,34]. In these studies, $Li_xNi_{0.75}Co_{0.25}O_2$

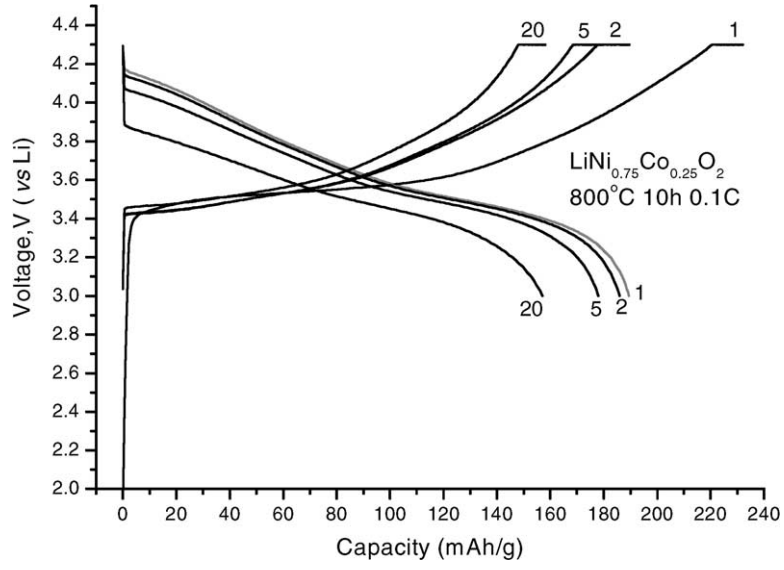

Fig. 5. Potential vs. capacity curves for the $LiNi_{0.75}Co_{0.25}O_2$ sample prepared at 800 °C.

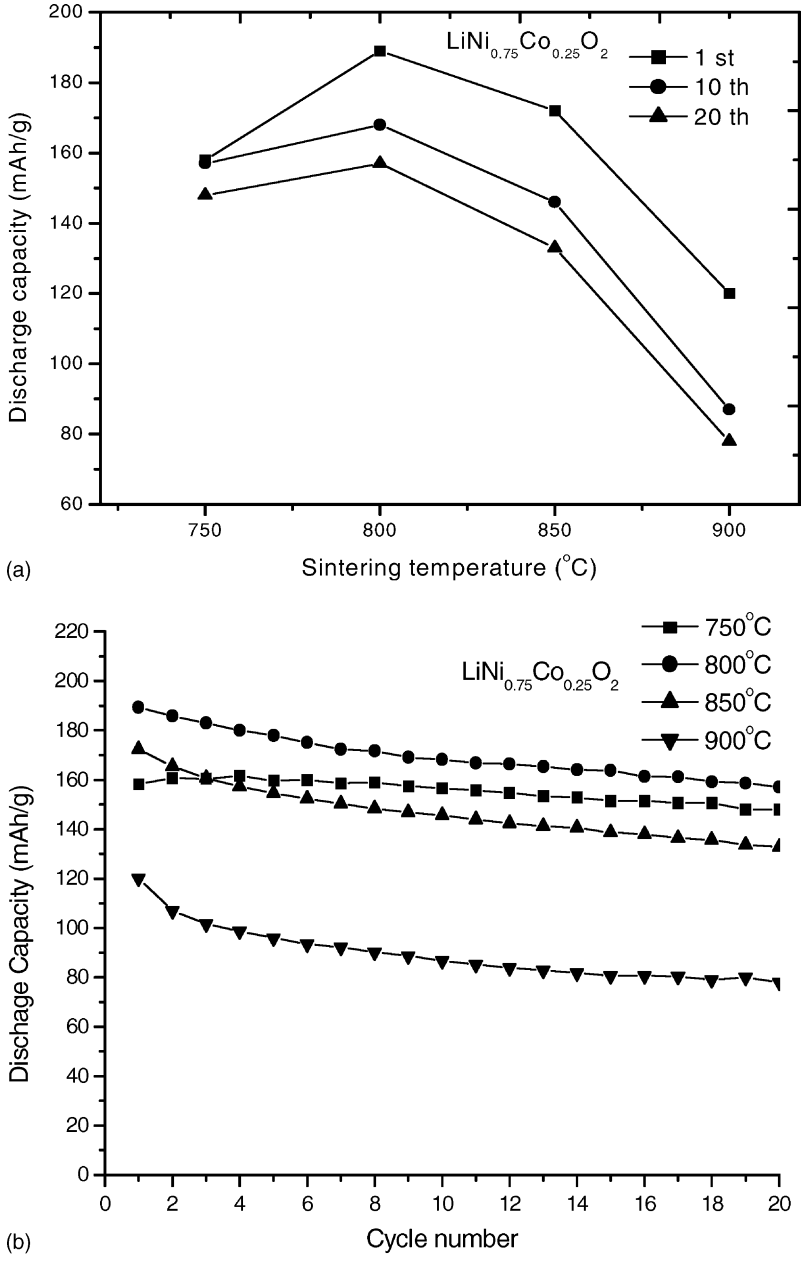

Fig. 6. (a) Discharge capacity as function of temperature for cycles 1, 10 and 20. (b) Discharge capacity as function of cycle number for $LiNi_{0.75}Co_{0.25}O_2$ sample prepared at different sintering temperatures.

Table 3
Selected electrochemical properties of $LiNi_{0.75}Co_{0.25}O_2$ at various sintering temperatures

Sintering temperature (°C)	1st Cycle CC (mAh g^{-1})	1st Cycle DC (mAh g^{-1})	Irreversible capacity (mAh g^{-1})	Percentage lost (%)	20th Cycle CC (mAh g^{-1})	20th Cycle DC (mAh g^{-1})	Irreversible capacity (mAh g^{-1})	Percentage lost (%)
750	188.8	158.3	30.5	16.2	148.4	147.9	0.5	0.3
800	232.0	189.3	42.7	18.4	158.1	157.0	1.1	0.7
850	214.1	172.3	41.8	19.5	134.3	132.8	1.5	1.1
900	194.9	120.2	74.7	38.3	80.5	78.0	2.5	3.1

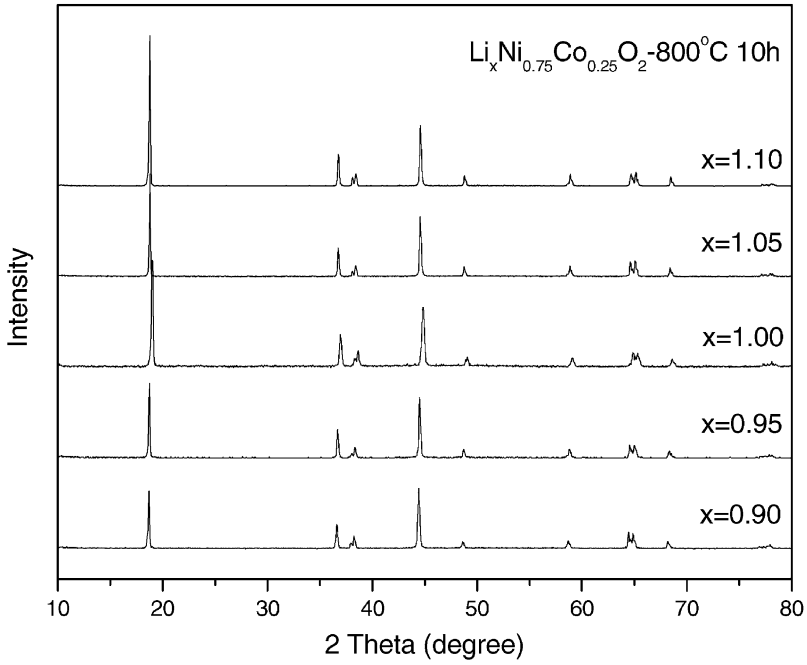

Fig. 7. XRD patterns for $Li_xNi_{0.75}Co_{0.25}O_2$ samples with different x-values prepared at 800 °C for 10 h.

was prepared with different lithium contents to determine the optimum lithium content to obtain excellent electrochemical performance from the material. The XRD patterns for $Li_xNi_{0.75}Co_{0.25}O_2$, where $x = 0.90$, 0.95, 1.00, 1.05 and 1.10, prepared by the sol–gel method at 800 °C for 10 h are shown in Fig. 7. The XRD spectra indicate that all the prepared samples have a typical layered structure with space group *R*3-*m*. No impurity-related peaks are observed in the XRD pattern for $Li_xNi_{0.75}Co_{0.25}O_2$. All the peaks are characteristic of $Li_xNi_{0.75}Co_{0.25}O_2$, as reported in the X-ray powder data file of JCPDS.

The variation of discharge capacity as a function of cycle number for $Li_xNi_{0.75}Co_{0.25}O_2$ material with different lithium contents is given in Fig. 8(a). It is clear that the first discharge capacities increase with increasing lithium content (x-value) from 0.90 to 1.05. Further increase in the lithium content to 1.10 decreases the discharge capacity. The charge and discharge capacities for selected cycles are listed in Table 4. The variation of discharge capacity with lithium content in the 1st, 10th and 20th cycles is presented in Fig. 8(b). The discharge capacities at different discharge cycles increase as the lithium content is increased. The discharge capacities have maximum values for the sample with $x = 1.05$. The discharge capacity then decreases as the x-value is increased to 1.10.

The superior electrochemical performance of the $Li_{1.05}Ni_{0.75}Co_{025}O_2$ material indicates that excess lithium is needed to saturate the available lithium sites. If the lithium sites are saturated, it is difficult for Ni^{2+} ions to occupy the lithium sites. In other words, site exchange is prevented in the case of excess lithium, and hence good hexagonal ordering and excellent electrochemical performance is obtained. If the lithium content is beyond the optimum level, however, it is possible that the lithium ions would also occupy the sites which are not available for lithium insertion and extraction processes, lithium diffusion may be restricted and hence the charge and discharge capacities are decreased.

Table 4
Charge and discharge capacities of $Li_xNi_{0.75}Co_{0.25}O_2$ for various lithium stoichiometries

Cycle	$Li_xNi_{0.75}Co_{0.25}O_2$									
	$x = 0.90$		$x = 0.95$		$x = 1.00$		$x = 1.05$		$x = 1.10$	
	CC	DC	CC	DC	CC	DC	CC	DC	CC	DC
1	199.8	164.2	200.0	171.8	232.0	189.3	227.7	206.1	217.8	197.3
2	164.8	165.8	172.5	172.1	189.5	185.8	206.7	200.4	197.3	193.4
5	167.2	166.0	172.2	170.9	179.7	177.9	190.8	187.3	186.1	182.9
10	162.9	161.0	167.1	166.2	168.9	168.2	178.9	176.0	172.6	169.6
20	153.1	150.7	157.0	155.6	158.1	157.0	163.2	161.9	152.5	150.1

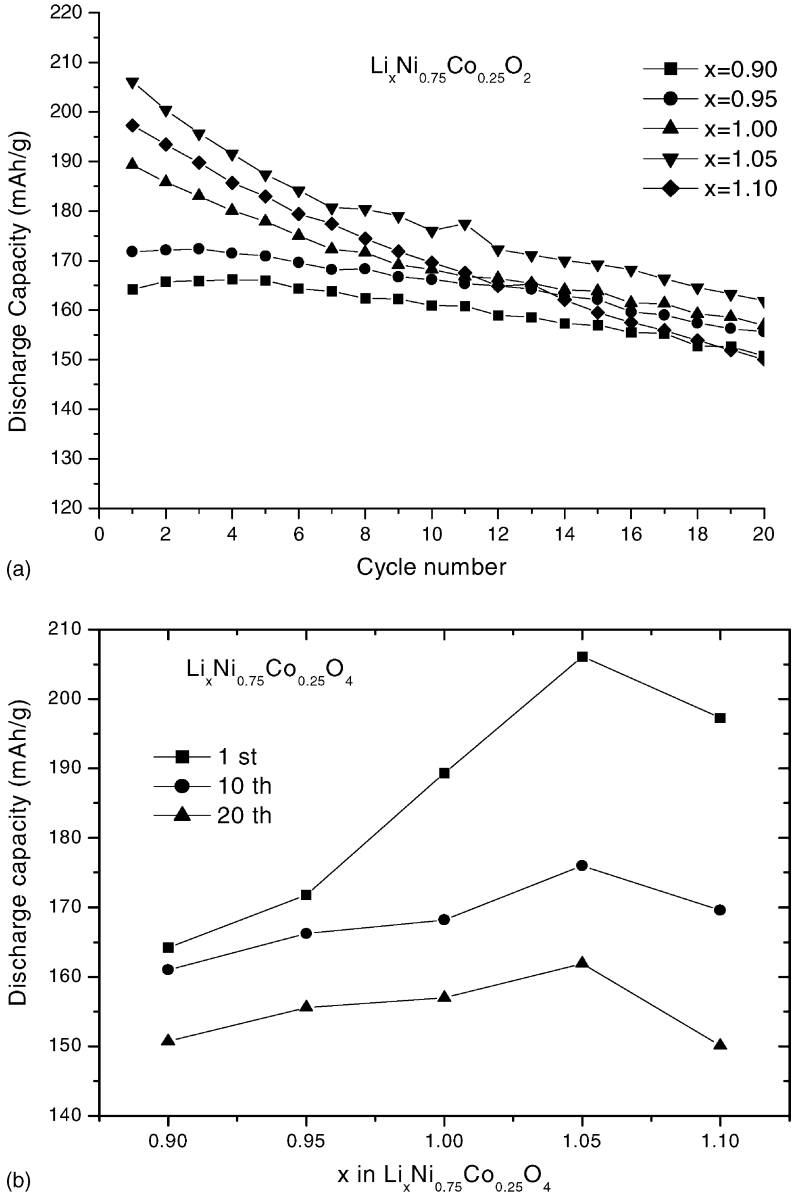

Fig. 8. (a) Discharge capacity vs. cycle number curves. (b) Discharge capacity as function of x-values at 1, 10 and 20 cycles of $Li_xNi_{0.75}Co_{0.25}O_2$ sample prepared at 800 °C for 10 h.

4. Conclusions

$LiNi_{1-y}Co_yO_2$ was prepared with different y-values by the sol–gel method with sintering at 800 °C for 10 h. X-ray diffraction patterns of the prepared samples reveal a hexagonal layered structure with a space group $R3$-m. The sample, $LiNi_{0.75}Co_{0.25}O_2$, sintered at 800 °C for 10 h yield the largest initial discharge capacity and shows the best electrochemical performance. It is believed that this is due to good hexagonal ordering and crystallinity, as well as relatively small and uniform particle size. In addition, it is found that the sample, $Li_{1.05}Ni_{0.75}Co_{0.25}O_2$, shows the better electrochemical performance among the samples prepared with different lithium content. This is ascribed to Ni^{2+} ions being prevented from occupying lithium sites.

Acknowledgements

The financial support from the National Science Council (NSC 89-2214-E-011-044 and NSC 90-2811-E-011-005), the Education Ministry (EX-91-E-FA09-5-4), the Chung-Shan Institute of Science and Technology, and the National Taiwan University of Science and Technology, Taiwan, ROC is gratefully acknowledged.

References

[1] T. Ohzuku, A. Ueda, Solid State Ion. 69 (1994) 201.
[2] M.G.S.R. Thomas, W.I.F. David, J.B. Goodenough, P. Groves, Mater. Res. Bull. 20 (1985) 1137.

[3] R. Kanno, H. Kubo, Y. Kawamoto, T. Kamiyama, F. Izumi, Y. Takeda, M. Takano, J. Solid State Chem. 110 (1994) 216.
[4] J.R. Dahn, U.V. Sacken, M.W. Juzkow, H. Al-Janaby, J. Electrochem. Soc. 138 (1991) 2207.
[5] M. Broussely, F. Perton, J. Labat, R.J. Staniewicz, A. Romero, J. Power Sources 43–44 (1993) 209.
[6] J. Morales, C. Perez, J.L. Tirado, Mater. Res. Bull. 25 (1990) 623.
[7] W. Li, J.N. Reimers, J.R. Dahn, Phy. Rev. B 46 (1992) 3236.
[8] G.G. Amatucci, J.M. Tarascon, L.C. Klein, J. Electrochem. Soc. 143 (1996) 1114.
[9] M. Broussely, P. Biensan, B. Simon, Electrochim. Acta 45 (1999) 3.
[10] K. Dokko, M. Nishizawa, S. Horikoshi, T. Itoh, M. Mohamed, I. Uchida, Electrochem. Solid State Lett. 3 (1999) 3.
[11] I. Saadoune, C. Delmas, J. Mater. Chem. 6 (1996) 193.
[12] C. Delmas, I. Saadoune, Solid State Ion. 53–56 (1992) 370.
[13] E. Zhecheva, R. Stoyanova, Solid State Ion. 66 (1993) 143.
[14] J.N. Reimers, J.R. Dalin, J. Electrochem. Soc. 139 (1992) 2091.
[15] C. Delmas, I. Saadoune, A. Rougier, J. Power Sources 43–44 (1993) 595.
[16] A. Alcantara, J. Morales, J.L. Tirado, R. Stoyanova, E. Zhecheva, J. Electrochem. Soc. 142 (1995) 3997.
[17] A. Hirano, R. Kanno, Y. Kawamoto, Y. Nitta, K. Okamara, T. Kamiyama, F. Izumi, J. Solid State Chem. 134 (1997) 1.
[18] R.K.B. Gover, M. Yonemura, A. Hirano, R. Kanno, Y. Kawamoto, C. Murphy, B.J. Mitchell, J.W. Richardson, J. Power Sources 81–82 (1999) 535.
[19] R. Alcantara, P. Lavela, J.L. Tirado, R. Stoyanova, E. Zhecheva, J. Electrochem. Soc. 145 (1998) 730.
[20] I. Saadoune, C. Delmas, J. Solid State Chem. 136 (1998) 8.
[21] Y. Fujita, K. Amine, J. Maruta, H. Yasuda, J. Power Sources 90 (2000) 82.
[22] R.K.B. Gover, R. Kanno, B.J. Mitchell, M. Yonemura, Y. Kawamoto, J. Electrochem. Soc. 147 (2000) 4045.
[23] C.C. Chang, N. Scarr, P.N. Kumta, Solid State Ion. 112 (1998) 329.
[24] J. Cho, B. Park, J. Power Sources 92 (2001) 35.
[25] Y.K. Sun, I.H. Oh, K.Y. Kim, J. Mater. Chem. 7 (1997) 1481.
[26] C. Julien, C. Letranchant, S. Rangan, M. Lemal, S. Ziolkiewicz, S. Castro-Garcia, L. El-Farh, M. Benkaddour, Mater. Sci. Eng. B 76 (2000) 145.
[27] E. Levi, M.D. Levi, G. Salitra, D. Aurbach, R. Oeston, U. Heider, L. Heider, Solid State Ion. 126 (1999) 97.
[28] B.J. Hwang, R. Santhanam, D.G. Liu, Y.W. Tsai, J. Power Sources 102 (2001) 326.
[29] B.J. Hwang, R. Santhanam, D.G. Liu, J. Power Sources 101 (2001) 86.
[30] Y. Gao, M.V. Yakovieva, W.B. Ebner, Electrochem. Solid State Lett. 1 (1998) 117.
[31] J.N. Riemers, E. Rossen, C.D. Jones, J.R. Dahn, Solid State Ion. 61 (1993) 335.
[32] J.R. Dahn, U.V. Sacken, C.A. Michel, Solid State Ion. 44 (1990) 87.
[33] B.D. Cullity, Elements of X-Ray Diffraction, 2nd ed., Addison-Wesley, Reading, MA, 1978, 102 pp.
[34] G.T.K. Fey, V. Subramanian, J.G. Chen, Electrochem. Commun. 3 (2001) 234.